Recessed-gate quasi-enhancement-mode AlGaN/GaN high electron mobility transistors with oxygen plasma treatment*

Yun-Long He(何云龙)[1], Chong Wang(王冲)[1,†], Min-Han Mi(宓珉瀚)[1], Xue-Feng Zheng(郑雪峰)[1], Meng Zhang(张濛)[2], Meng-Di Zhao(赵梦荻)[1], Heng-Shuang Zhang(张恒爽)[1], Li-Xiang Chen(陈立香)[2], Jin-Cheng Zhang(张进成)[1], Xiao-Hua Ma(马晓华)[1,2], and Yue Hao(郝跃)[1,2]

[1] *Key Laboratory of Wide Band Gap Semiconductor Materials and Devices, School of Microelectronics, Xidian University, Xi'an* 710071, *China*
[2] *School of Advanced Materials and Nanotechnology, Xidian University, Xi'an* 710071, *China*

(Received 15 June 2016; revised manuscript received 17 August 2016; published online 30 September 2016)

In this paper, the enhancement-mode AlGaN/GaN HEMT combined with the low damage recessed-gate etching and the optimized oxygen plasma treatment was fabricated. Scanning electron microscope/energy dispersive spectrometer (SEM/EDS) method and x-ray photoelectron spectroscopy (XPS) method were used to confirm the formation of oxides. Based on the experimental results, the obtained enhancement-mode HEMT exhibited a threshold voltage of 0.5 V, a high peak transconductance of 210 mS/mm, and a maximum drain current of 610 mA/mm at the gate bias of 4 V. Meanwhile, the on/off current ratio of enhancement-mode HEMT was as high as 10^8, drain induced barrier lowering (DIBL) was as low as 5 mV/V, and subthreshold swing (SS) of 80 mV/decade was obtained. Compared with the conventional HEMT, the Schottky reverse current of enhancement-mode HEMT was three orders of magnitude lower, and the off-state breakdown voltage of which was higher. In addition, a power gain cutoff frequency (f_{max}) of the enhancement-mode HEMT was larger than that of the conventional one.

Keywords: AlGaN/GaN, high electron mobility transistors, recessed-gate, oxygen plasma

PACS: 73.40.Kp, 81.05.Ea, 85.30.De, 85.30.Tv **DOI:** 10.1088/1674-1056/25/11/117305

1. Introduction

Since GaN materials have high electron saturation velocities and high breakdown electric fields, AlGaN/GaN high electron mobility transistors (HEMTs) are widely used in the field of high frequency and high power.[1,2] In order to meet the AlGaN/GaN HEMT applications in the field of radio frequency (RF) switch circuits and digital circuits, enhancement-mode AlGaN/GaN HEMTs become an important choice. There are many methods to fabricate enhancement-mode AlGaN/GaN HEMTs, of which the recessed-gate structure is proved to be a feasible way. Enhancement-mode HEMTs using recessed-gate structure usually have the following several methods: the first method is an etching groove under the gate region only using dry etching.[3] This method is simple, but the etching depth is significant, so the damage induced by etching is severe and the Schottky leakage current will increase. The second way is an etching groove using dry etching to make the barrier layer thickness minimized or be completely etched, then a better quality dielectric layer is grown above the gate region.[4,5] This method can obtain a large threshold voltage, and a small Schottky reverse leakage current. However, this method is more difficult to precisely control the etching depths, and the etching damage in the channel will be introduced with a thin barrier layer. Meanwhile, the quality of interface between barrier layer and gate dielectric is difficult to be guaranteed. The third one is using wet etching to form the groove under the gate region, and then a better quality dielectric layer is grown above the gate region.[6] Using this way, the etching depth can be precisely controlled, but the process is time consuming and the lateral extension under the gate region cannot be ignored.

In this paper, enhancement-mode AlGaN/GaN HEMTs combined with the low damage recessed-gate structure and optimized oxygen plasma treatment were fabricated. By using this method, the AlGaN barrier layer was less etched and the distance between gate and channel was large enough to avoid the etching damage in the channel by etching. Oxygen plasma treatment can make part of the AlGaN barrier layer be oxidized, which can form the simple metal–insulator–semiconductor (MIS) structure. Scanning electron microscope/energy dispersive spectrometer (SEM/EDS) and x-ray photoelectron spectroscopy (XPS) were used to confirm the formation of oxides. This process is relatively simple. The enhancement-mode HEMT with this method exhibits high performance in the terms of direct current (DC) and RF.

2. Experimental methods

The AlGaN/GaN material wafer was grown on sapphire substrate by metal–organic chemical vapor deposition. The epitaxial layers consist of (from the substrate to the surface): 400-μm sapphire, 2-μm non-doped GaN layer,

*Project supported by the National Natural Science Foundation of China (Grant Nos. 61574110, 61334002, and 61474091) and the National Key Technology Research and Development Program of the Ministry of Science and Technology of China (Grant No. 2015AA016801).

†Corresponding author. E-mail: chongw@xidian.edu.cn

© 2016 Chinese Physical Society and IOP Publishing Ltd

and 18-nm $Al_{0.25}Ga_{0.75}N$ barrier layer. The room temperature Hall measurements of the structure yield an electron sheet density of 9.2×10^{12} cm^{-2} and an electron mobility of 1800 cm$^2\cdot$V$^{-1}\cdot$s^{-1}.

The fabrication processes started with ohmic contacts formed by an alloyed Ti/Al/Ni/Au metal stack annealed at 830 °C for 30 s, and then the mesa was formed by using Cl_2 plasma dry etching in an inductively coupled plasma (ICP) system. After SiN deposition of 60 nm on the surface by plasma enhanced chemical vapor deposition, the SiN above the gate region was etched by the ICP system. Then the wafer was divided into three regions: A, B, and C. There was no treatment on region A. Region B was only treated by Cl_2 plasma in the ICP system, during which the etch rate was 0.14 nm/s and the etching depth was 7 nm. Region C was not only treated by Cl_2 plasma in the ICP system, and then region C was treated by O_2 plasma in the ICP system. The ICP coil power was 100 W, the reflected RF power was 30 W, and the treatment time was 60 s. The gate electrode of the whole wafer was formed by the Ni/Au (30 nm/200 nm) E-beam evaporation and liftoff. The gate length of 1.2 μm, and source drain spacing of 3 μm were set in the three types of devices. The Keithley 4200 semiconductor parameter analyzer and Agilent E8363B vector network analyzer were used to measure the device parameters. The regions A, B, and C for three types of devices were named samples A, B, and C, respectively. The cross-sectional schematics of these three types of post gated HEMTs and an electron-microscope image of enhancement-mode HEMT are shown in Fig. 1.

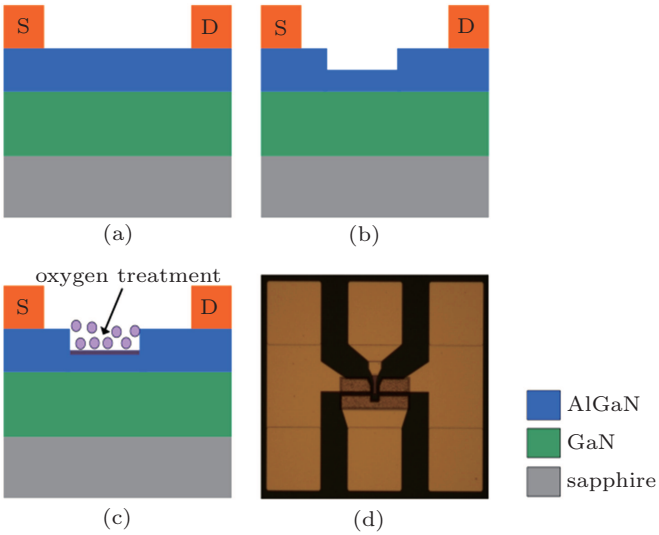


Fig. 1. (color online) (a) Cross-sectional schematic of sample A, (b) cross-sectional schematic of sample B. (c) Cross-sectional schematic of sample C, (d) electron-microscope image of enhancement-mode HEMT.

3. Results and discussion

Figure 2 shows the typical AFM images with 5 μm×5 μm scan area of the surfaces for three samples. The surface roughnesses in terms of root mean square (RMS) for samples A, B, and C are 0.65 nm, 0.93 nm, and 1.43 nm, respectively. It can be seen that the surface roughness is increased after treating Cl_2 plasma, but the increment is no more than 0.3 nm indicating the low damage of the recess-gate. While compared with the surface roughness of sample A, that of sample C has increased 0.78 nm, which is related to greater RF power by oxygen plasma treatment.

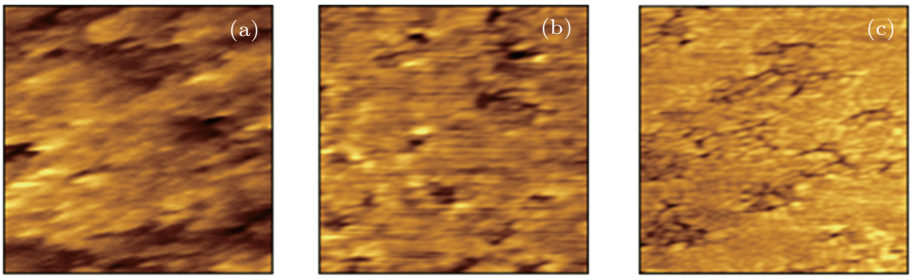


Fig. 2. (color online) AFM images of the surfaces for three samples. (a) Sample A, (b) sample B, (c) sample C.

Figure 3 shows the typical transfer characteristics of three samples at $V_{DS} = 10$ V. The threshold voltage (V_{th}) is defined as the gate bias intercept of the linear extrapolation of the drain current from the point of peak transconductance in transfer curves. The threshold voltage of sample A is about −2.5 V and that of sample B is about −1.2 V, that of sample C is 0.5 V. The AlGaN barrier layer thickness is reduced by etching, so the electron concentration in the channel is reduced.[7] The distribution of the carriers can be deduced from the capacitance–voltage (C–V) curves, as shown in Fig. 4. The AlGaN barrier layer thickness of sample A is 18 nm, that of sample B is 11 nm, and that of sample C is 9 nm. AlGaN barrier layer thickness under the gate region is reduced by 2 nm by oxygen plasma treatment. Therefore, the reduction of AlGaN barrier thickness is one of the reasons for the threshold voltage positive drift of sample C.

It can be seen that the channel current of sample C at $V_{GS} - V_{th} = 2$ V is 410 mA/mm and that of sample B at $V_{GS} - V_{th} = 2$ V is 420 mA/mm. It indicates that under the same gate drive voltage, two-dimensional electron gas (2DEG) con-

centration under the gate region after oxygen plasma treatment is not significantly changed, the current has little degradation. The peak transconductance of sample A is 177 mS/mm and that of sample B is 218 mS/mm. The higher peak transconductance of recess-gate HEMTs is related with the fact that the AlGaN barrier layer is thin under the gate region. Sample C shows the peak transconductance of 215 mS/mm, which indicates that the ability of gate control of HEMTs by oxygen plasma treatment is not significantly degraded.

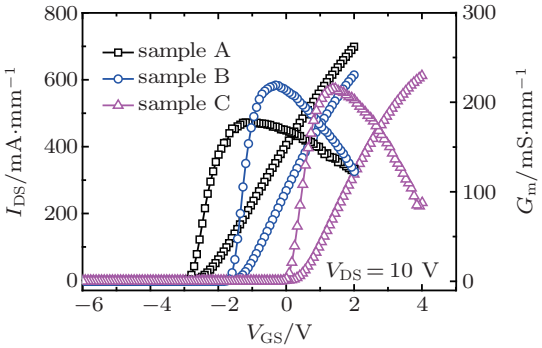


Fig. 3. (color online) Transfer characteristics of three samples.

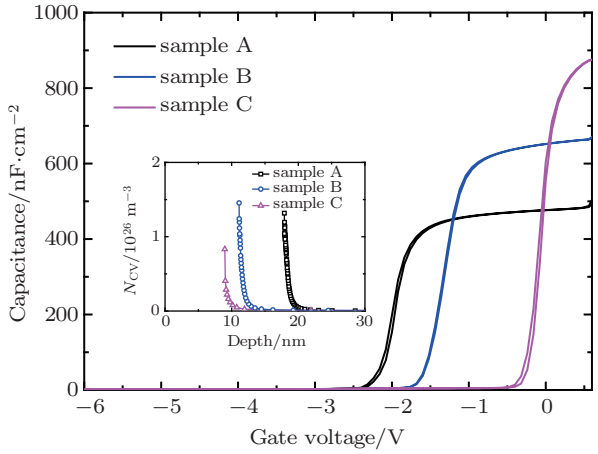


Fig. 4. (color online) Capacitance–voltage measurement of three samples.

Saito *et al.*[8] have studied the influence of the etching depth of recessed-gate on AlGaN/GaN HEMT characteristics. The relationship between the threshold voltage and AlGaN barrier layer thickness under the gate region can be expressed as

$$V_{th} = \phi_B + \frac{qN_{2D}}{\varepsilon}(t_{CRG} - t_{RA}), \quad (1)$$

$$t_{CR} = \frac{E_D - \Delta E_C}{qN_{2D}}, \quad (2)$$

where E_D is the surface level at the AlGaN barrier layer, ΔE_C is the conduction band discontinuity, N_{2D} is the 2DEG density at the non-recessed region, ϕ_B is the Schottky barrier height, ε is the dielectric constant for the AlGaN layer, t_{RA} is the AlGaN layer thickness at the recessed region, and t_{CR} is the critical AlGaN barrier thickness while normalized 2DEG density is exactly equal to 0. Assuming $E_D = \phi_B$, the relationship between V_{th} and t_{RA} is linear. The equation $V_{th} = 0.843–0.1857t_{RA}$ can be obtained by the calculation, the threshold voltage corresponding 9-nm AlGaN barrier layer should be -0.82 V, however, the threshold voltage of 0.5 V is obtained with a 9-nm AlGaN barrier layer by oxygen plasma treatment. As a result, the threshold voltage positive drift has other factors.

In order to study the mechanism for threshold voltage variations by oxygen plasma treatment, the SEM/EDS and XPS methods are used. The SEM/EDS method can be used to analyse the surface element changes, and XPS can scan and measure the chemical structure within 8 nm depth. Two specimens are obtained, one specimen has no treatment, and the other one is treated by oxygen plasma in the ICP system. The ICP coil power is 100 W, the RF power is 30 W, and the treatment time is 60 s. As shown in Fig. 5(a), the peaks of C, O, N, Ga can be seen in the non-treated specimen, the peak of element O appears due to the natural oxidation. After the oxygen plasma treatment, the peak intensity of O increases significantly and the percentage of oxygen atoms varies from 2.46% to 5.59% (more than doubled). Due to the presence of background noise and measurement errors, the peak intensity of Ga has a little change, the variation of Ga is low enough to be ignored. It can be inferred that, O_2 and Al of the AlGaN barrier layer can be bonded. Figure 5(b) shows the XPS data of two specimens. As can be seen, the specimen without any treatment has an Al–N bond and Al–O bond, but the content of the Al–O bond is low, the formation of Al–O bond is related to the natural oxidation. However, compared with the specimen without treatment, the intensity of the Al–O bond in the specimen by oxygen plasma treatment is higher. This is proved that more Al element of AlGaN barrier layer in the specimen by oxygen plasma treatment can be oxidized, and the MIS structure can be formed.[9] This can reduce the content of Al component in the AlGaN barrier layer and further reduce the polarization effect of the barrier layer and deplete channel electrons.

Figure 6 shows the transfer characteristics of three samples under Semi-logarithmic coordinates system. The I_{DS} of samples A and B are 10^{-5} mA/mm and 10^{-4} mA/mm in the off-state, respectively. However, the I_{DS} of sample C is as low as 10^{-6} mA/mm in the off-state, and the on/off current ratio of sample C is as high as 10^8. The off-state leakage current of sample B being larger than that of sample A may be due to the etching damage. Oxygen plasma treatment can reduce the content of the Al component in the AlGaN barrier layer and form the MIS structure, this can reduce 2DEG concentration under the gate region and the direct tunneling of electrons can be suppressed. So the off-state leakage current of sample C decreases two orders of magnitude than that of sample B.

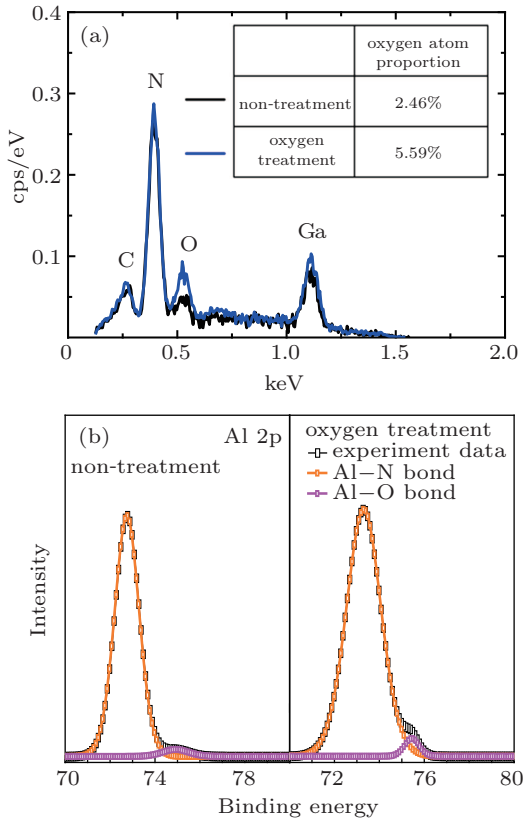


Fig. 5. (color online) The SEM/EDS acquisition rate and XPS results for two specimens (a) EDS data and (b) Al 2p core-level spectra.

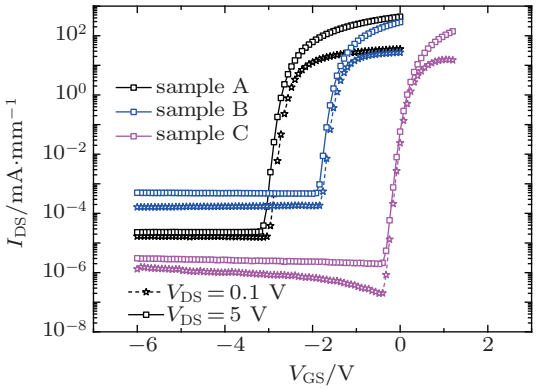


Fig. 6. (color online) Transfer current of three samples under Semi-logarithmic coordinate system.

When the device is biased at different drain voltage, the threshold voltage will drift due to the drain induced barrier lowering (DIBL) effect and the short channel effect. The rate of change of threshold voltage drift and drain-source voltage is usually used to measure the short channel effect.[10] It can be seen from Fig. 6, the DIBL of sample A is 37 mV/V, that of sample B is 16 mV/V, while the DIBL of sample C is 5 mV/V which is a small value. The small value of DIBL of sample C may be related to that the AlGaN barrier layer thickness is reduced and the ability of being gate-controlled is enhanced. In addition, it is noticed that the subthreshold swing (SS) of sample C is 80 mV/decade.

In order to study the influence of recessed gate etching and oxygen plasma treatment on the interface state, double sweep *C–V* curves at 100 kHz frequency of three samples are tested, as shown in Fig. 4. Due to the small area of devices' Schottky region, Schottky barrier diodes (SBDs) which have a larger Schottky region are selected. There is no obvious difference in hysteresis among three samples, indicating low concentration of surface states under the gate region by plasma treatment.[11] It is evident that a sharper rise is seen from the depletion mode to the accumulation mode obtained from sample C compared to that obtained on sample A. This indicates that, compared with sample A, sample C has less interface states and oxygen plasma treatment can effectively improve the interface quantity.[12]

Figure 7 shows the Schottky reverse leakage current for three samples. The Schottky reverse leakage current of sample A reaches 10^{-8} A/mm, and the Schottky reverse leakage current of sample B increases by an order of magnitude than that of sample A. However, the Schottky reverse leakage current of sample C is decreased by two orders of magnitude than that of sample B, reaching 10^{-9} A/mm. There are three mechanisms for Schottky reverse leakage current.[13] The increase of the Schottky reverse leakage current of sample B mainly has two factors: one is the thin AlGaN barrier thickness increasing the probability of direct tunneling; the other is that the production of recessed gate brought a certain etching damage which could increase the probability of trap-assisted tunneling. However, by the *C–V* hysteresis curve, it can be observed that the surface states introduced by etching damage are very small. Therefore, the direct tunneling is the major factor for the Schottky reverse leakage current of the recessed gate device increasing. The thickness of the AlGaN barrier layer by oxygen plasma treatment can be further reduced, and the probability of direct tunneling increases further. However, the Schottky reverse leakage current of sample C is decreased by three orders of magnitude than that of sample B. It is attributed to the MIS layer which is formed on the surface of the AlGaN barrier by oxygen plasma treatment.

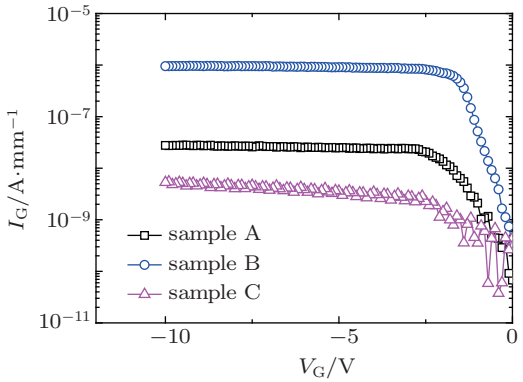


Fig. 7. (color online) Gate leakage current for three samples.

On the one hand, oxygen plasma treatment can make the Al composition in the AlGaN barrier layer reduce, and the electrons density below the gate is also decreased. On the other hand, the MIS layer can increase the barrier height that can suppress the probability of direct tunneling, and the oxygen plasma treatment does not introduce significant surface states. Therefore, the probability of trap-assisted tunneling is not possible, and the Schottky reverse leakage current by oxygen plasma treatment is suppressed.

Figure 8 shows the breakdown characteristics of three samples. In this paper, the drain bias which corresponds to the drain current reaching 1 mA/mm is considered to be the breakdown voltage. As can be seen from Fig. 8, there is little difference on the breakdown voltage between sample A and sample B, the breakdown voltage of them is about 160 V, which indicates that there is low damage in gate recess etching. After oxygen plasma treatment, due to the formation of the A–O bond, the MIS structure will be introduced between the gate and AlGaN barrier layer. The electron concentration of sample C decreases more significantly under the off-state condition and the Schottky reverse leakage current is reduced, the avalanche breakdown could be suppressed under the off-state condition. So the breakdown voltage of the sample C is larger than that of sample A and sample B.

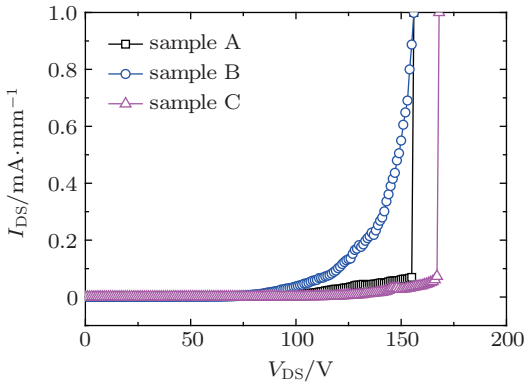


Fig. 8. (color online) The off-state breakdown characteristics of three samples.

The on-wafer RF performance of three samples with $L_G = 1.2$ μm is characterized from 100 MHz to 16 GHz. The current gain cutoff frequency (f_T) is given by the extrapolation of $|h_{21}|^2$ with a −20 dB/dec slope. The current gain and maximum stable gain (MSG) of three samples are derived from measured S parameters as a function of frequency, as shown in Fig. 9. For sample A, f_T of 7 GHz and a power gain cutoff frequency (f_{max}) of 18 GHz are obtained at $V_{DS} = 10$ V and $V_{GS} = -1.3$ V. For sample B, f_T of 7.1 GHz and f_{max} of 17 GHz are obtained at $V_{DS} = 10$ V and $V_{GS} = -0.5$ V. For sample C, f_T of 7.3 GHz and f_{max} of 20 GHz are obtained at $V_{DS} = 10$ V and $V_{GS} = 1.2$ V. It can be seen that there are little differences on f_T among three samples, f_{max} of sample C is the largest. f_{max} can be expressed as[14]

$$f_{max} = \frac{f_T}{2\sqrt{\dfrac{(R_i + R_s + R_g)}{R_{ds}} + (2\pi f_T) R_g C_{gd}}}, \tag{3}$$

where f_T is the current-gain cutoff frequency and C_{gd} is the gate-drain (depletion region) capacitance, while R_i, R_s, R_g, and R_{ds} represent the gate-charging, source, gate, and output resistance, respectively. As known that R_{ds} is related to the short channel effect, good gate controlled ability leading the larger R_{ds}. After oxygen plasma treatment on the gate region, due to the combination of oxygen and Al such that the thickness of AlGaN barrier layer under the gate region is reduced. The gate controlled ability of sample C will be improved, R_{ds} will increase, so f_{max} of sample C is increased.

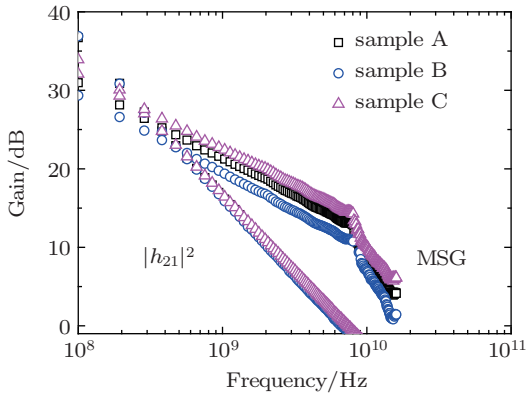


Fig. 9. (color online) RF performance of three samples.

4. Conclusion

In summary, high performance enhancement-mode AlGaN/GaN HEMTs have been fabricated. This method combines the low damage recessed-gate structure and optimized oxygen plasma treatment. The increment of RMS is no more than 0.3 nm indicating the low damage of recess-gate through AFM test. SEM/EDS method and XPS method are used to confirm the formation of oxides. The obtained enhancement-mode HEMTs exhibit threshold voltage of 0.5 V, high peak transconductance of 210 mS/mm, and maximum drain current of 610 mA/mm at a gate bias of 4 V. Meanwhile, the on/off current ratio of enhancement-mode HEMTs is as high as 10^8, DIBL is as low as 5 mV/V, and SS of 80 mV/decade is obtained. Compared with the conventional HEMTs, the Schottky reverse current of enhancement-mode HEMTs is three orders of magnitude lower and the off-state breakdown voltage of which is higher. In addition, f_{max} of enhancement-mode HEMTs is larger than that of the conventional one. The results indicate that the low damage recessed-gate structure combined with the optimized oxygen plasma treatment can be a favorable way to fabricate the enhancement-mode HEMTs.

References

[1] Zheng J X, Ma X H, Lu Y, Zhao B C, Zhang H H, Zhang M, Cao M Y and Hao Y 2015 *Chin. Phys. B* **24** 107305

[2] Lee D S, Gao X, Guo S P, Kopp D, Fay P and Palacios T 2011 *IEEE Electron Dev. Lett.* **32** 1525

[3] Lanford W B, Tanaka T, Otoki Y and Adesida I 2005 *Electron. Lett.* **41** 449

[4] Wang Q P, Jiang Y, Zhang J Q, Kawaharada K, Li L, Wang D J and Ao J P 2015 *Semicond. Sci. Technol.* **30** 065004

[5] Zhou Q, Chen B W, Jin Y, Huang S, Wei K, Liu X Y, Bao X, Mou J Y and Zhang B 2015 *IEEE Trans. Electron Devices* **62** 776

[6] Tang C, Xie G and Sheng K 2015 *IEEE* 27*th International Symposium on Power Semiconductor Devices & ICs (ISPSD)*, May 12, 2015, Hong Kong, China, p. 233

[7] Binari S C, Ikossi K, Roussos J A, Kruppa W, Park D, Dietrich H B, Koleske D D, Wickenden A E and Henry R L 2001 *IEEE Trans. Electron Devices* **48** 465

[8] Saito W, Takada Y, Kuraguchi M, Tsuda K and Omura I 2006 *IEEE Trans. Electron Devices* **53** 356

[9] Zhang K, Chen X, Mi M H, Zhao S L, Chen Y H, Zhang J C, Ma X H and Hao Y 2015 *Phys. Status Solidi A* **212** 1081

[10] Zanandrea A, Bahat-Treidel E, Rampazzo F, Stocco A, Meneghini M, Zanoni E, Hilt O, Ivo P, Wuerfl J and Meneghesso G 2012 *Microelectron Reliab.* **52** 2426

[11] Miczek M, Mizue C, Hashizume T and Adamowicz B 2008 *J. Appl. Phys.* **103** 104510

[12] Feng Q, Tian Y, Bi Z W, Yue Y Z, Ni J Y, Zhang J C, Hao Y and Yang L A 2009 *Chin. Phys. B* **18** 3014

[13] Karmalkar S, Satyan N and Mahaveer S D 2006 *IEEE Electron Dev. Lett.* **27** 87

[14] Chung J W, Hoke W E, Chumbes E M and Palacios T 2010 *IEEE Electron Dev. Lett.* **31** 195